# Book of Mormon Central

General Geology

Author(s): Jerry D. Grover, Jr.
Source: *Geology of the Book of Mormon*
Published: Vineyard, UT: n.p., 2014
Page(s): 19–50

# Chapter 3
# **General Geology**

The purpose of this book is not to give a detailed description of all of the geologic information available for the Isthmus of Tehuantepec, but rather to provide sufficient information to describe the geology related to the destruction described in 3$^{rd}$ Nephi. Also, as non-scientists will be interested in this work, the geologic information is presented in simpler terms than one might find in a scientific journal.

The explanation of volcanoes and many earthquakes is found in the geologic theory of 'plate tectonics,' which involves numerous plates that comprise the outer layer of the earth and move around because of forces in the more liquid mantle upon which the plates sit. Tectonic plates include the oceanic crust and the thicker continental crust.

Since the various plates are moving, along their boundaries they are either colliding with other plates, separating from other plates, or sliding alongside other plates. Boundaries where they are colliding are referred to as 'convergent'; where they are separating, the boundaries there are referred to as 'divergent.' Along convergent boundaries, one plate will typically go underneath the other, which is called 'subduction.' Subduction carries plates down into the mantle; the material lost is roughly balanced by the formation of new (oceanic) crust along divergent margins by spreading, which usually occurs on the seafloor. In this way, the total surface area of the globe remains the same.
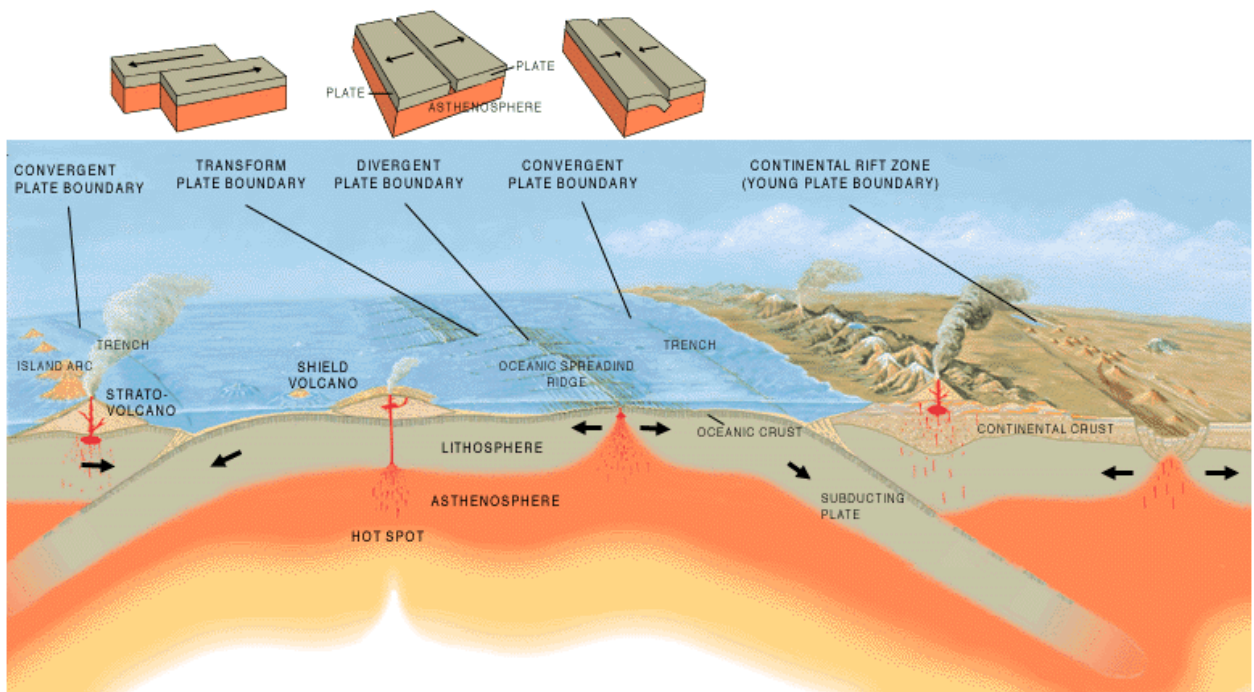


**Figure 6.** Cross section of plate tectonic model

As a plate is subducted it eventually melts as it enters the mantle. Sediments or rocks that are lighter will melt and form magma, which will migrate back up into the continental crust of the plate under

which it is moving. Not all of this magma will make it to the surface in a liquid form, but when it does, a volcano or lava field results. In a divergent plate boundary, magma also comes to the surface and forms an oceanic ridge. There are other areas called 'hot spots' where magma can also come to the surface and form volcanoes. Hawaiian volcanoes are the result of a hot spot. A theoretical diagram showing a cross-section of plate tectonics is shown in figure 6.

In the case of the Isthmus of Tehuantepec, the Cocos Plate, which lies to the south and west, is being subducted underneath both the Caribbean Plate and North American Plate at certain locations, creating a string or group of volcanoes, which are called 'volcanic arcs' (see figure 7).
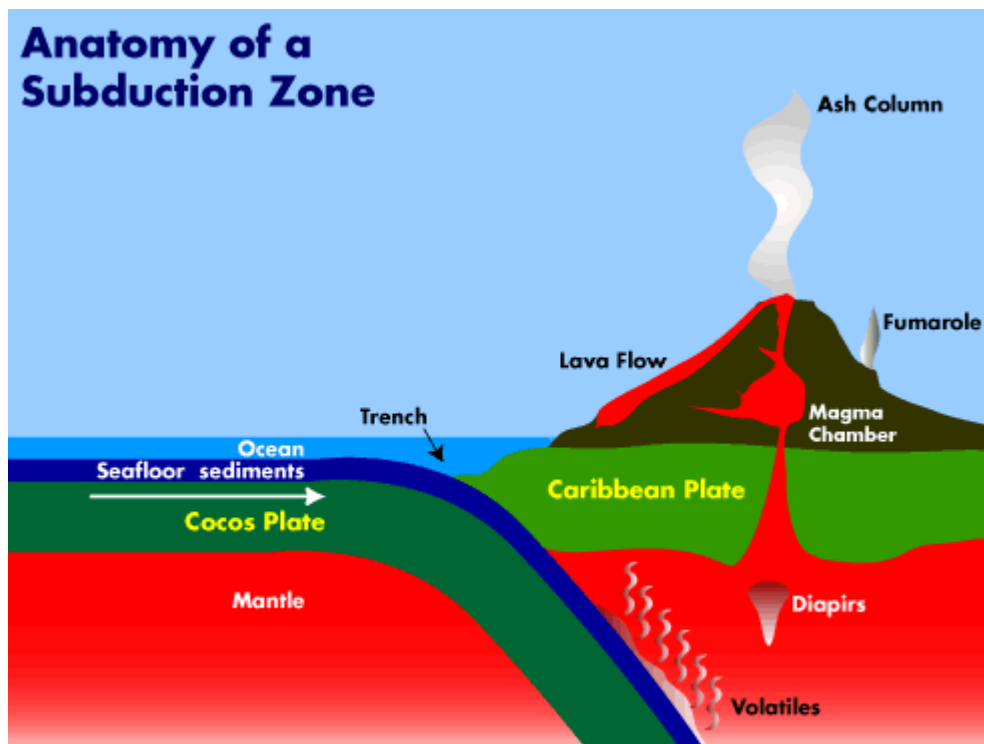


**Figure 7.** Typical subduction zone at the Isthmus of Tehuantepec

The subduction of the Cocos Plate underneath the Caribbean and North American plates is not uniform in the angle of subduction. When subduction occurs under two plates along their boundary the situation becomes complex. In addition, there appears to be some rifting or divergence underneath the west side of the Isthmus that complicates the formation of the volcanic areas and which types of magma and volcanoes form. Scientists do not appear to have reached consensus on exactly what is occurring here. Figure 8 shows a bird's-eye view of the Cocos plate subduction process going on at the Isthmus. The pink areas are the different volcanic arcs or areas. They are labeled with abbreviations as follows:

CMVB:  Central Mexican Volcanic Belt

MCVA:  Modern Chiapanecan Volcanic Arc

CAVA:  Central America Volcanic Arc

MAT:  Middle America Trench

Los Tuxtlas:  The Tuxtla Volcanoes are often referred to as the Tuxtla Volcanic Field (TVF)

TMVB:  Trans-Mexican Volcanic Belt

As geology is a three-dimensional science, in that one has to determine the situation underneath the surface of the earth as well as at the surface, geologists use what are called 'cross-sections' as depictions. Figure 8 shows four separate lines, A to A', B to B', C to C', and D to D'. If one imagines making a slice down through the earth along one of the lines and imagines looking at the cut section from the side, one would see what is shown in figure 8. This would be similar to cutting through a layered cake and looking at the slice from the side.
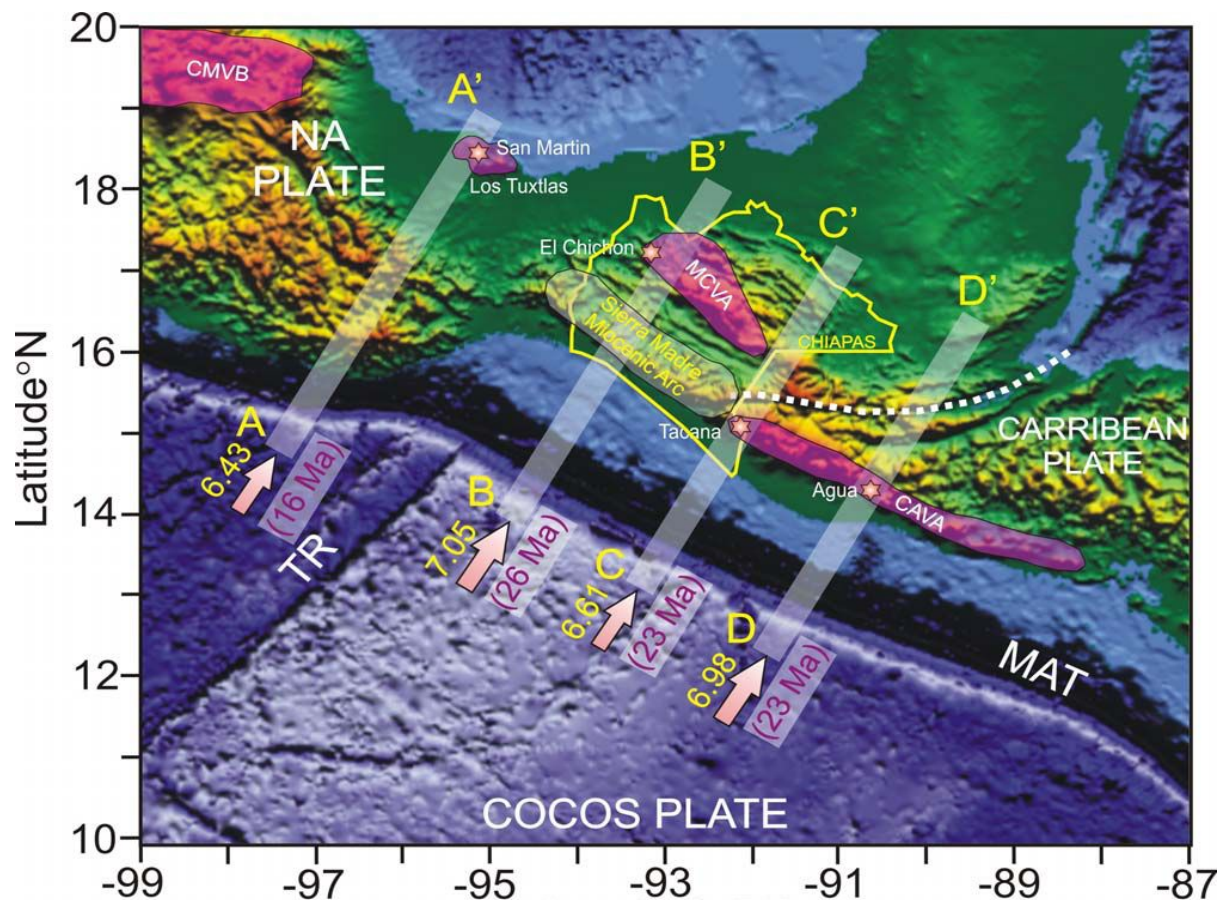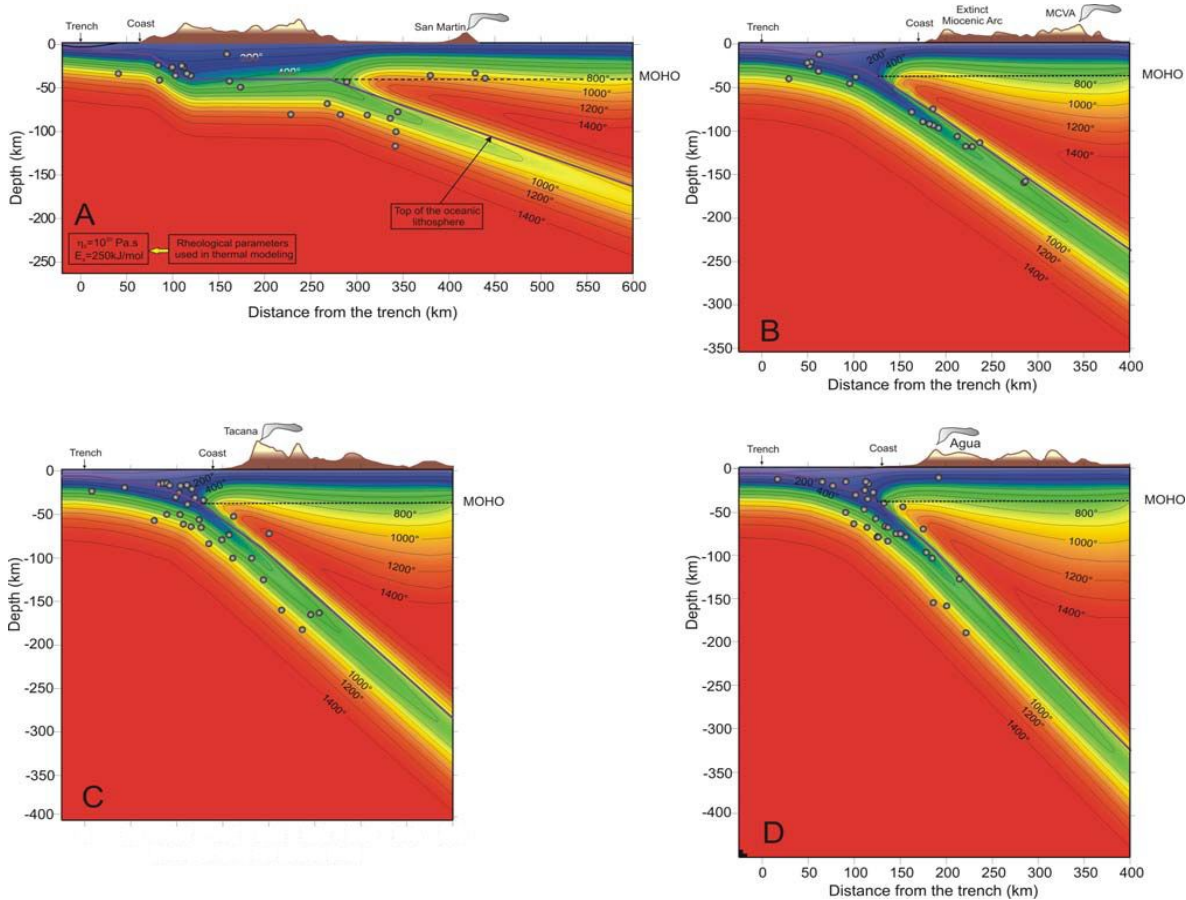
**Figure 8.** Cocos Plate subduction and volcanic arcs or belts and cross-sections (Manea and Manea, 2006, 29–30)

## Isthmus of Tehauntepec Fault Zones Earthquakes

Figure 9 shows that the geology in the Isthmus becomes a bit more complicated because it not only involves the subduction of the Cocos plate, but also involves the relationship and boundary movement between the North American and Caribbean Plates. While somewhat of an oversimplification, the North American and Caribbean Plates are sliding alongside of each other to some extent, with the North American Plate rotating and sliding to the west and northwest and the Caribbean Plate sliding to the east. Figure 9 contains arrows that show the direction of movement, indicating the direction of movement of the plates. As is evident, it is a bit messy, as some areas are not sliding but are actually undergoing compression (arrows pointing directly at each other) while some other areas are undergoing tension (arrows pointing directly away from each other).
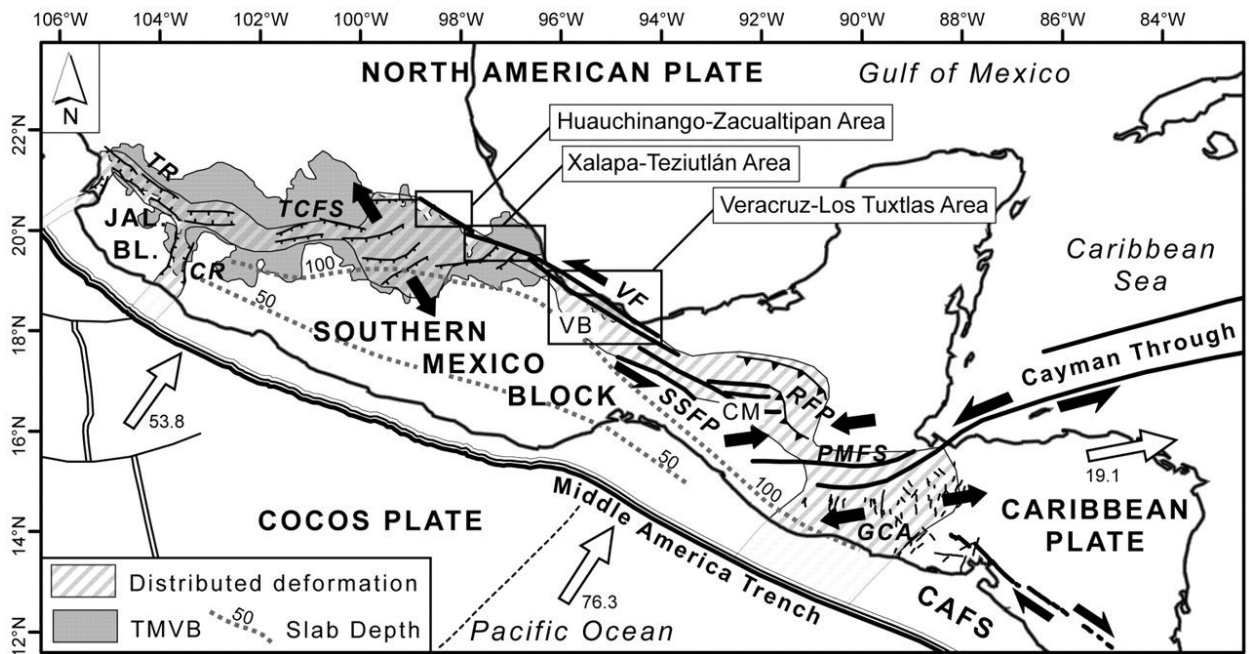
**Figure 9.** General geologic structure map of the Isthmus of Tehuantepec (Andreani et al., 2008)

At this juncture it would be useful to discuss the general nature of faults. There are three kinds of faults, strike-slip (lateral), normal (block), and reverse (thrust) fault (see figure 10). All three of these types of faults are present in the Isthmus of Tehuantepec.
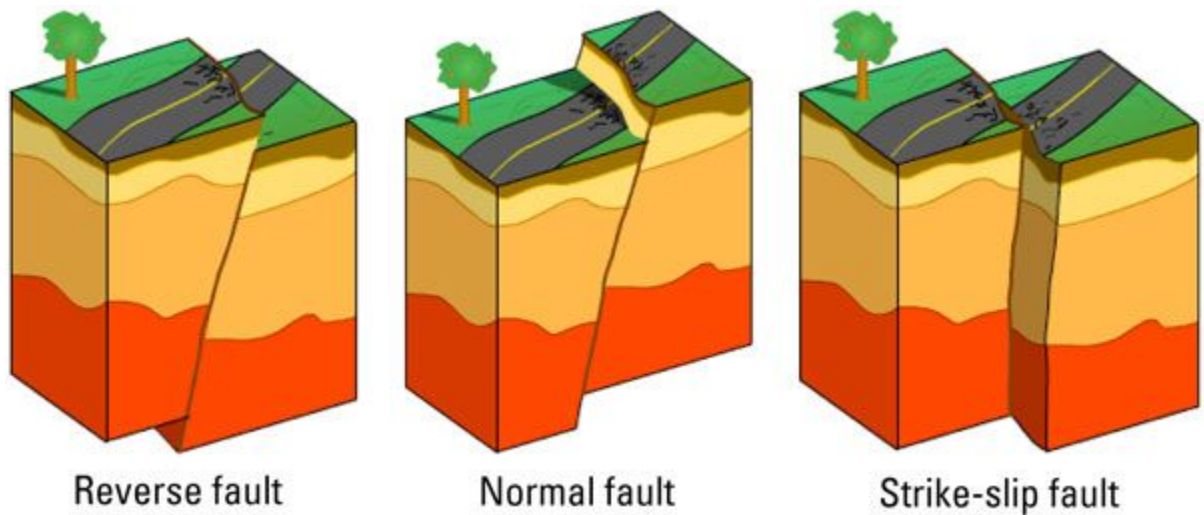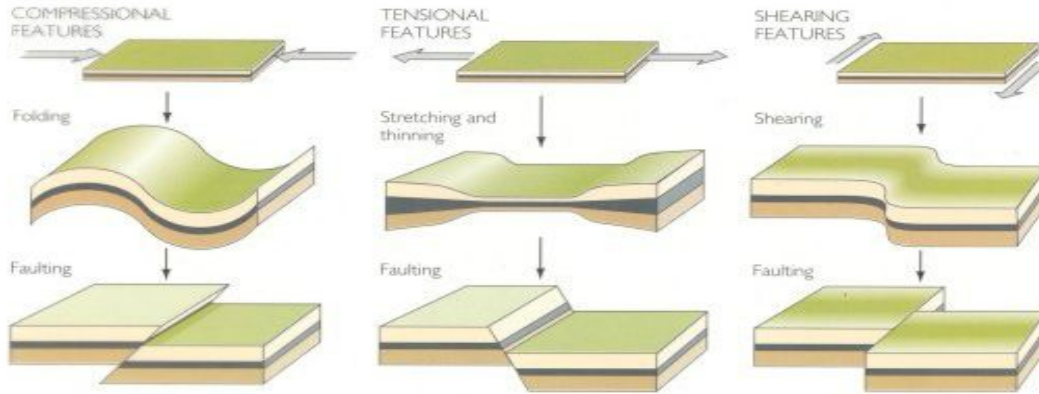


**Figure 10.** Types of faults

The type of faulting that occurs depends on the type of pressure or tension that is being exerted on that particular section of the earth's crust. The earth's crust responds to the differing pressure environments by folding or fracturing. Figure 11 displays the typical folding and fracture responses.

**Figure 11.** Crustal response to compression, tension, and shearing pressure

There are two main zones or provinces of regional faulting in the Isthmus of Tehuantepec. Figure 12 shows the principal areas of faulting and recent (in geologic time) earthquake activity with earthquakes exceeding a magnitude of 4. The different colors show the depths of the earthquakes. The figure also shows blue and white "beach balls," which are figures that geologists use as a convenient 2D way to depict the 3D type and movement of a given fault. These "beach balls" are depictions of what is called the focal mechanism. Figure 13 shows the types of faults that each of the "beach balls" represent.

**Figure 12.** Locations of shallow (< 30 km) and Ms > 4 earthquakes outlining the main plate boundaries (Andreani et al., 2008)
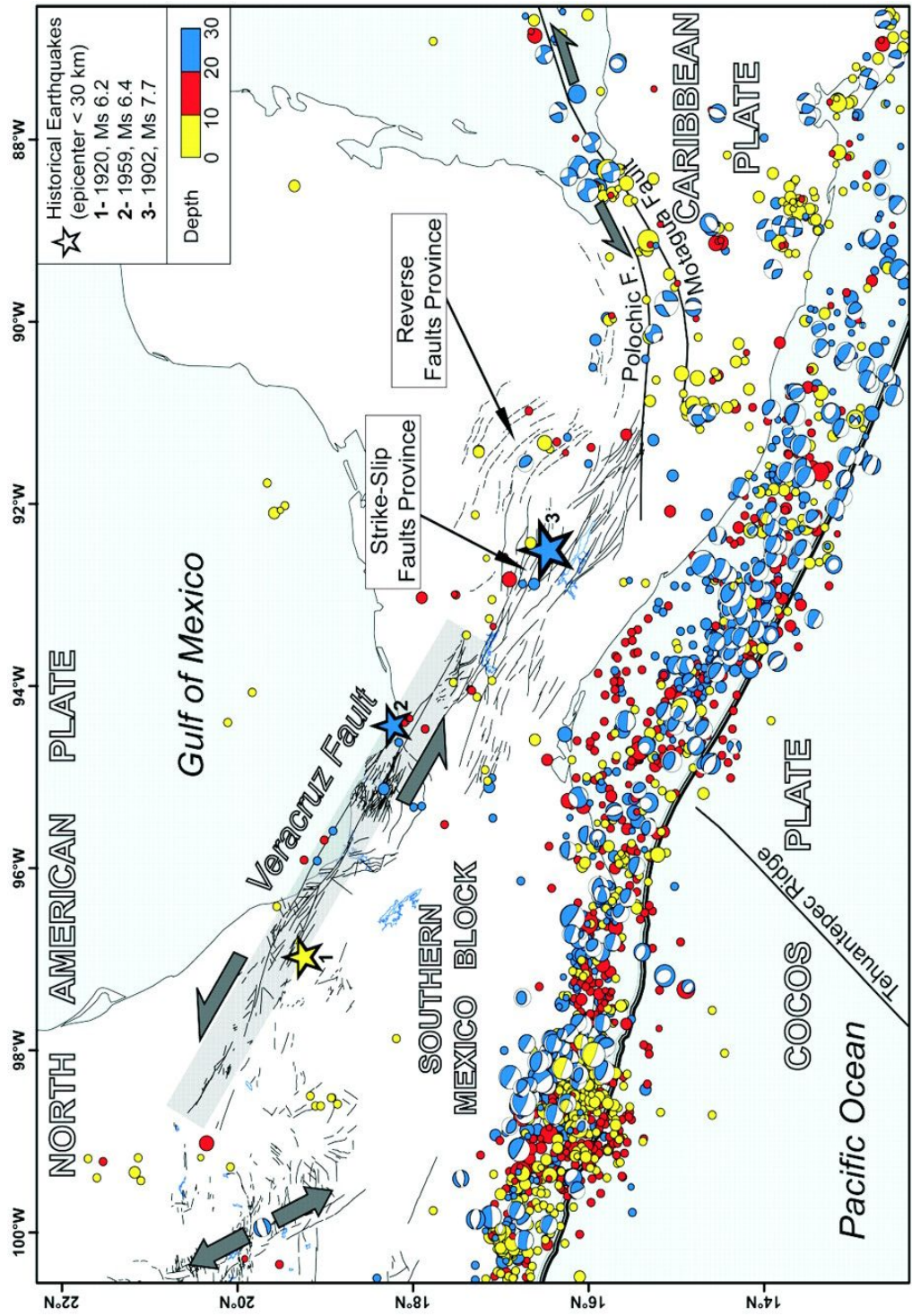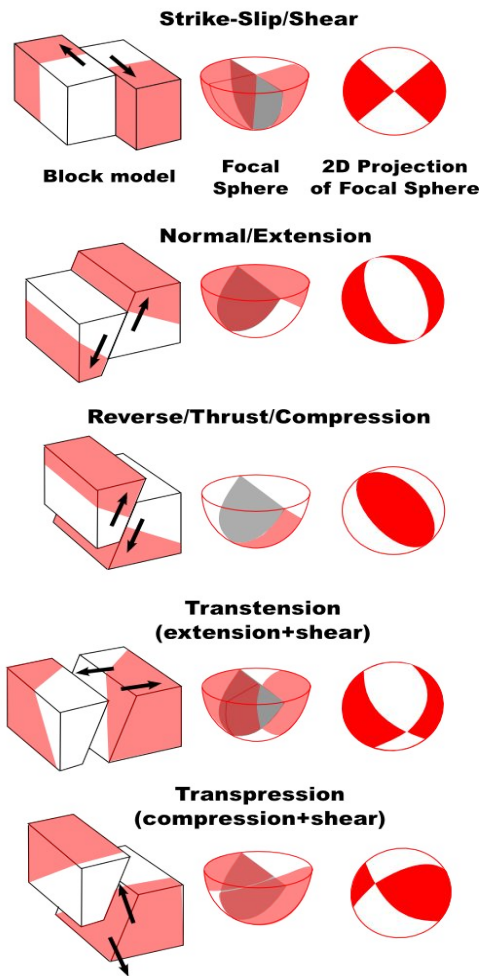
**Figure 13.** Focal mechanism depictions

## Pacific Coast Subduction Fault

The first faulting area, and the most active zone, is along the Pacific Coast where the Cocos Plate is being subducted. This area consists principally of compressional faulting at depth along the subduction zone, with surface faults being normal faults with some strike-slip elements. Many of these faults may be deep faults with little or no surface expression. As a general rule, in the subduction zone shallow earthquakes are nearer subduction trenches and get deeper as the plate is further subducted. Shallow faulting at the earth's surface above the subduction zone away from the trench typically contains normal and to a lesser extent, strike-slip faulting. It should be noted that in both fault provinces, all three types of faults are typically present, the province is classified for the general regional pressure regime and the most dominant types of active faults.

Veracruz-Polochic/Motogua Strike-Slip Fault System

As indicated in figures 9 and 12, there is a long active strike-slip fault system that runs from the northwest to the southeast through the Isthmus of Tehuantepec. It does not produce near the number of earthquakes as the Pacific Coast Subduction area, however it does produce large shallow earthquakes periodically. The northwest end of the fault zone transitions into a tensional fault system. The province consists of the main Veracruz fault system that runs southeast through the neck of the isthmus, with a transition step-over area consisting of numerous strike-slip offset faults before it connects with the main Polichic/Motagua strike-slip segment to the south. There is an area of reverse faulting northwest and adjacent to the central strike-slip transition area.

## Isthumus of Tehuantepec Volcanoes

Each of the Isthmus volcanic arcs, belts, and fields has multiple volcanoes, volcanic cones, and lava flows. Figure 14 shows the location of the principal volcanoes. Some of these volcanoes are no longer active and were not active during Book of Mormon times. This factor will be used to narrow down the list of potential volcanoes that may have been involved in the 3$^{rd}$ Nephi catastrophe.
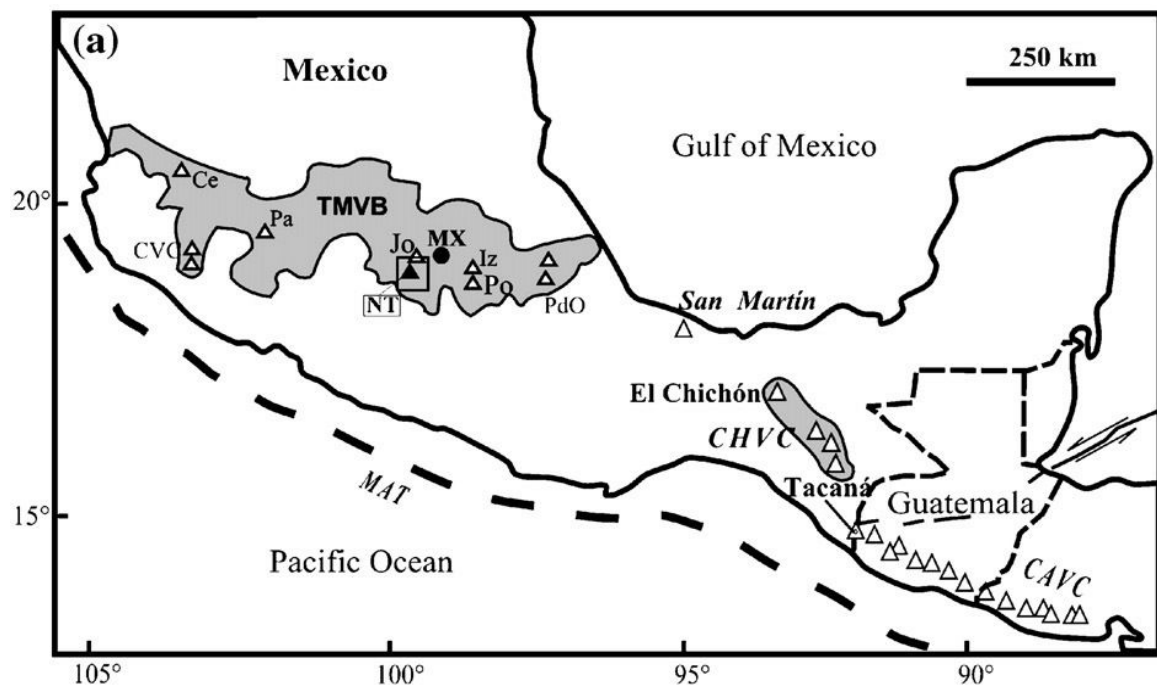


**Figure 14.** Volcano locations (triangles) in Southern Mexico and Guatemala (Bellotti et al., 2006)

Before commencing a discussion of individual volcanoes, it is necessary to delineate some general systems used in the classification of volcanoes and volcanic eruptions. There are a variety of systems and methods to classify volcanoes. This book will just present a few of the basic systems. The first classification of volcanoes is related to the shape and to some extent the type of the magma source. There are many varieties of compositions of magma, however, one of the principal parameters of magma that influence the volcano form and the nature of the eruption is the viscosity of the magma.

Viscosity means a fluid's ability to flow. A fluid that has high viscosity flows very slowly, like cold honey, whereas a fluid with low viscosity flows easily, such as water. Magma that has low viscosity produces lava that flows easier and thus produces thinner and flatter deposits like the fissure and shield volcanoes shown in figure 15. Some volcanoes form and erupt only once; they are called monogenetic volcanoes. For the most part, the volcanoes that will be discussed in this book are not monogenetic, but have erupted and formed various levels of layered deposits on their flanks like the composite volcano shown in figure 15.
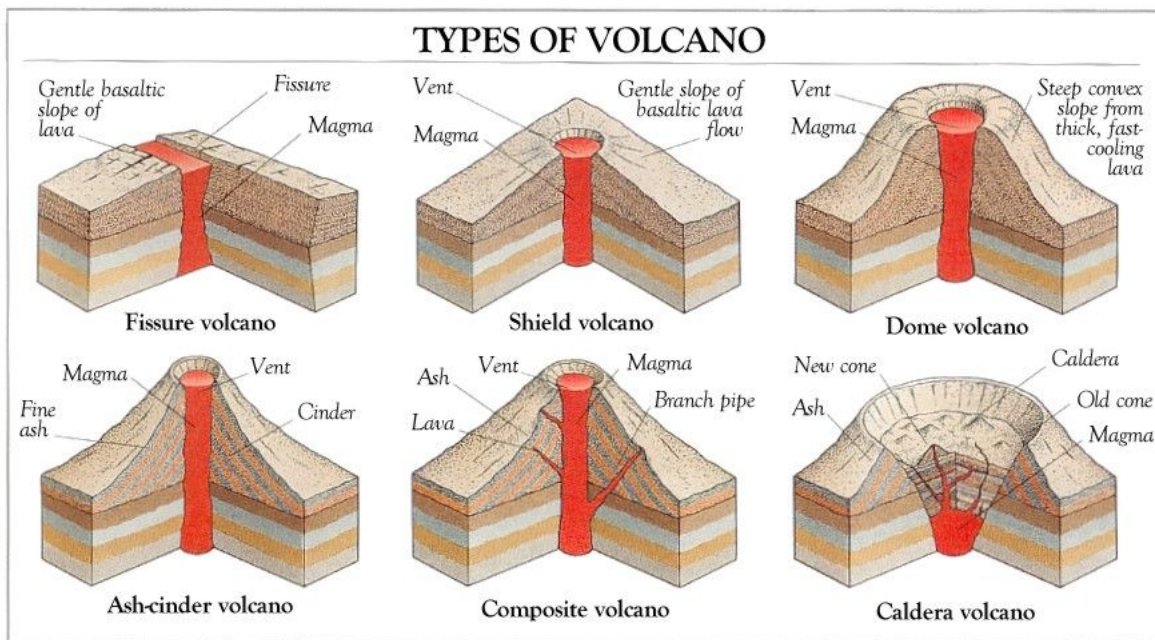


**Figure 15.** Volcano forms

Volcanic eruptions are classified both by their form and by their explosive power. The eruption forms are illustrated in figure 16. Keep in mind that these are just general forms; each volcano and each volcanic eruption is unique, and some volcanoes can exhibit more than one type of eruption. The power of a volcanic eruption is classified using the Volcanic Explosive Index or VEI, which consists of a numbering system from 0 to 8 with 8 being the most explosive. Figure 17 is a chart that shows the VEI scale and how the VEI generally relates to other features of volcanoes.

The nature in which material is expelled from a volcano also has different names and descriptions. The common types are shown in figure 18. Pyroclastic flows are especially deadly as they consist of superheated volcanic ash and volcanic rocks debris that travels at high speed, generally along the ground surface (see figure 19). Lahar flows occur where water is present, either in the form of snow, rain, groundwater, or surface streams and rivers (see figure 20). In a lahar the volcanic ash and other volcanic materials combine with the water and form a heavy mud that has the consistency of concrete slurry. These are also extremely deadly as they can contain huge amounts of material, travel quickly, and follow drainage channels through which the volcanic materials travel well beyond the obvious eruption area. Volcanoes generate fragmentary debris, everything from large house-size boulders to finely crushed rock material, to magma explosively sprayed in a mist of molten droplets and fragmentary glass and crystals. The term 'ejecta' is used for anything blasted out of an exploding

volcano. The term 'tephra' describes air fall ejecta and typically includes blocks, bombs, and lapilli (gravel sized material) that fall back to earth; these are referred to as ballistic particles. Tephra also includes ash and dust that become entrained in the air and spend time drifting, generally windborne, before falling back to the surface.
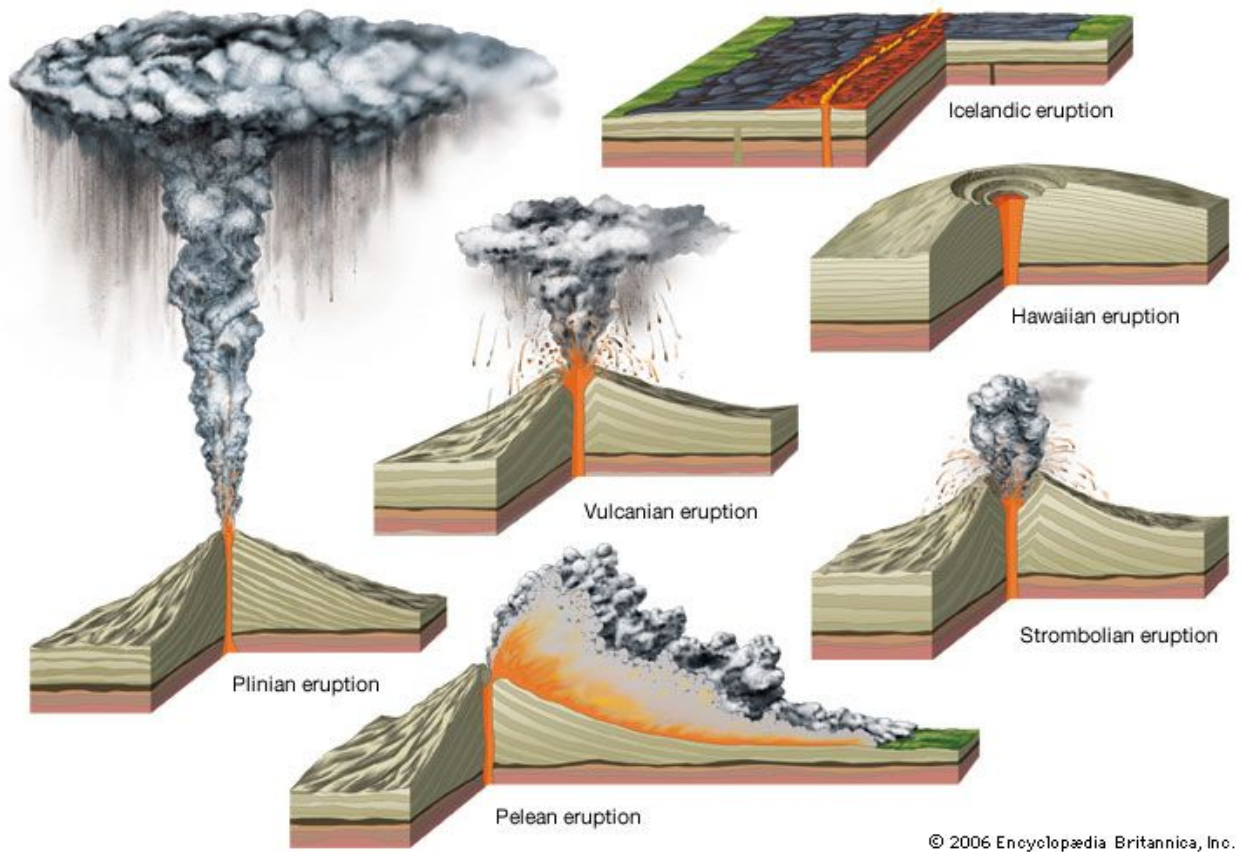


**Figure 16.** Volcanic eruption forms (courtesy Encyclopedia Britannica, 2006)

| VEI | 0 | 1 | 2 | 3 | 4 | 5 | 6 | 7 | 8 |
|---|---|---|---|---|---|---|---|---|---|
| General Description | Non-Explosive | Small | Moderate | Moderate-Large | Large | Very Large | | | |
| Volumn of Tephra (m³) | 1x10⁴ | 1x10⁶ | 1x10⁷ | 1x10⁸ | 1x10⁹ | 1x10¹⁰ | 1x10¹¹ | 1x10¹² | |
| Cloud Column Height (km) Above crater Above sea level | <0.1 | 0.1-1 | 1-5 | 3-15 | 10-25 | ← >25 → | | | |
| Qualitative Description | "Gentle," | "Effusive" ← "Explosive" → | | ← "Cataclysmic," "paroxysmal," "colossal" → ← "Severe," "violent," "terrific" → | | | | | |
| Eruption Type (see fig. 7) | | ← Strombolian → ← Hawaiian → | | ← Plinian → ← Vulcanian →← Ultra-Plinian → | | | | | |
| Duration (continuous blast) | | ← <1 hr → | | ← >12 hrs → ← 1-6 hrs → ← 6-12 hrs → | | | | | |
| Maximum explosivity | Lava flow Dome or mudflow | ← Phreatic → | | ← Explosion or Nuée ardente → | | | | | |
| Tropospheric Injection | Negligible | Minor | Moderate | Substantial → | | | | | |
| Stratospheric Injection | None | None | None | Possible | Definite | Significant → | | | |
| Eruptions | 976 | 1239 | 3808 | 1083 | 412 | 168 | 50 | 6 | 0 |

**Figure 17.** Volcanic explosive index chart



**Figure 18.** Volcanic deposition types
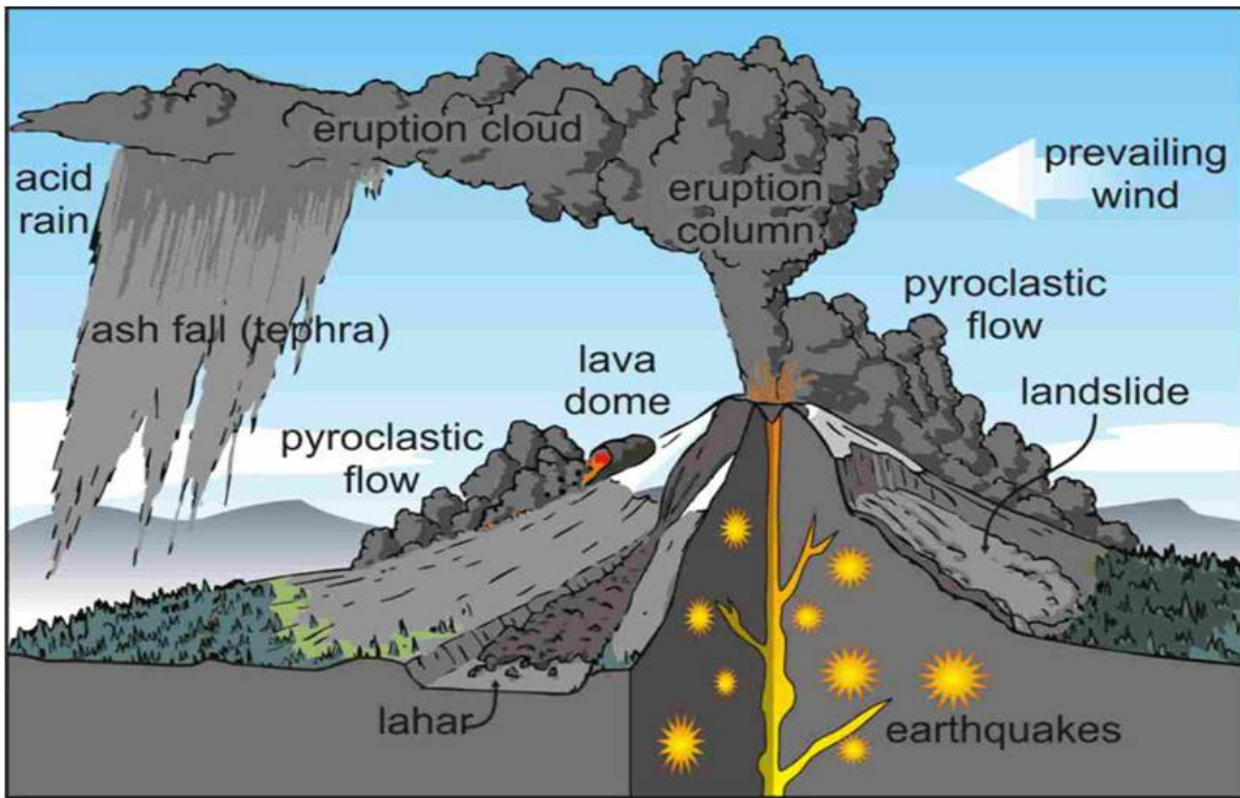
**Figure 19.** Pyroclastic flow from the 1991 Mount Pinatubo eruption (courtesy Wikipedia.org)



**Figure 20.** Lahar flow from the 1982 eruption of Galunggung, Indonesia (courtesy Wikipedia.org)

Volcanoes also emit large volumes of gases during eruptions, the bulk consisting of water, carbon dioxide, and sulfur and sulfur oxides. Very minor amounts of helium and halogens are also present.

# Individual Volcanoes in the Isthmus

Each of the volcanoes within the Isthmus will be briefly discussed. Volcanoes located in the land northward that have activity during Book of Mormon times will be discussed in greater depth. It is important to note that the historical volcanic eruption data will invariably be incomplete. It is clear after a review of the literature that the rainy semi-tropical climate of the Isthmus has eroded and obliterated many of the volcanic deposits, even those as old as just a few hundred years. In addition, subsequent eruptions cover up evidence of prior eruptions. Finally, some of the volcanoes have not had thorough geological investigations to differentiate historical volcanic deposits. There may be other eruptive events during the period of 3$^{rd}$ Nephi that are yet to be discovered, or whose evidence is no longer present.

It needs to be noted that for nearly all of the historic eruptions, the method used for confirmation of the date ranges is radiocarbon dating based on atmospheric amounts of $^{14}$C. As with any other sampling and laboratory method, there are possibilities for error, so care needs to be taken when a particular eruption date is supported by a single sample. Generally speaking, for purposes of this book, unless otherwise noted, the assumption is made that the radiocarbon date has been established using a sample that has been replicated to what scientists call the ±2σ level, for which there is a 95.% chance that the date lies within the date ranges given. Some sources did not list the level of accuracy of the sample data, so further investigation may be expected to modify those results. Of course, this level of accuracy is for the lab results, there can be errors that occur in the original sample. In addition to error from contamination of the sample, volcanoes, whether active or apparently dormant, produce carbon dioxide gas that can skew radiocarbon dating because they locally dilute the atmosphere with carbon that has no $^{14}$C activity, which local vegetation may have absorbed prior to burial (Bowman, 1990, 26).

This is not to imply that radiocarbon dates are not accurate in volcanic environments, but it does suggest that the more samples that are taken the better, and that there may be data disagreements among scientists on the same volcano that may only be resolved by looking for correspondence from other types of sampling or historical sources. The volcanic eruption of the Xitle volcano, which covered the city of Cuicuilco near Mexico City, is a perfect example. The site may have been tested more than any other volcanic site in the Americas, yet the radiocarbon dating by different archeaologists has swung in a range of 2500 years (Gonzalez et al. 2000, 218). It is best to keep an open mind on the identification of 3$^{rd}$ Nephi volcano(s) when considering radiocarbon dating of eruptions as a parameter.

## Volcanoes in the Land Northward

For purposes of this book, volcanoes beyond the Mexico City basin at a distance of 600 kilometers from the boundary of the land northward and the land southward are not considered, as the distance would seem to be too great to be relevant to the Book of Mormon area; furthermore, the Sorenson model doesn't have any discussions of sites beyond that boundary. The volcanoes for which the current data showed activity at or close to the 3$^{rd}$ Nephi time frames are shown on figures 21, 22, and 23 with red labels; those that were historically active but with insufficient data to show activity in the 3$^{rd}$ Nephi time frames are delineated with pink labels. Detailed discussions will only be made for volcanoes with documented eruptions within the 3$^{rd}$ Nephi time frames.

**Figure 21.** Northernmost volcanoes



**Figure 22.** Volcanoes located near the boundary of the land northward and the land southward

1. San Martín volcano (Tuxtla Volcano Complex)

The San Martín Volcano is a massive alkaline shield volcano located in the land northward and the flanks of the volcano extend to the Gulf of Mexico (see figure 23). It is elongated in a NW–SE direction and is capped by a 1-km-wide summit crater. The upper part of the 1650-m-high volcano is

covered with dense tropical rain forests. The summit and flanks of San Martín are dotted with more than 250 pyroclastic cones and maars. Well-preserved cinder cones are abundant between the summit of the volcano and Laguna Catemaco on the SE flank. The San Martín volcano is located on the northwest end of the volcanic complex, which consists of other inactive volcanoes to the southwest.

It is the highest peak within the Tuxtla Volcanic Field (TVF), also known as Los Tuxtlas Volcanic Field or Los Tuxtlas Massif, which consists of hundreds of cinder cones, maars, and three additional large volcanic edifices mostly dormant since late Pliocene: Santa Marta, San Martín Pajapan, and Cerro el Vigía. A maar is a broad, low-relief volcanic crater that is caused by a phreatomagmatic eruption, which is an explosion caused by groundwater coming into contact with hot lava or magma (see figure 24). A cinder or scoria cone is a steep conical hill of tephra (volcanic debris) that accumulates around and downwind from a volcanic vent (see figure 25).

A phreatomagmatic eruption is produced by flash vaporization of water due to rapid energy transfer from the magma by superheating. These eruptions began suddenly, without any warning activity (e.g., felt seismicity).



**Figure 23.** San Martín Volcano (Smithsonian, 2014)

**Figure 24.** Maar crater in the Pinacates Mountains near Rocky Point Mexico



**Figure 25.** Example of a cinder cone volcano in Parícutin, Mexico

The San Martín volcano is located directly on the lineament of the Veracruz fault system (see figure 26). A detailed geologic structural map shows the extent to which the San Martín volcanism is related

to the Veracruz fault structure (see figure 27). Eruption patterns generally follow the direction of the fault traces that make up the Veracruz fault system.
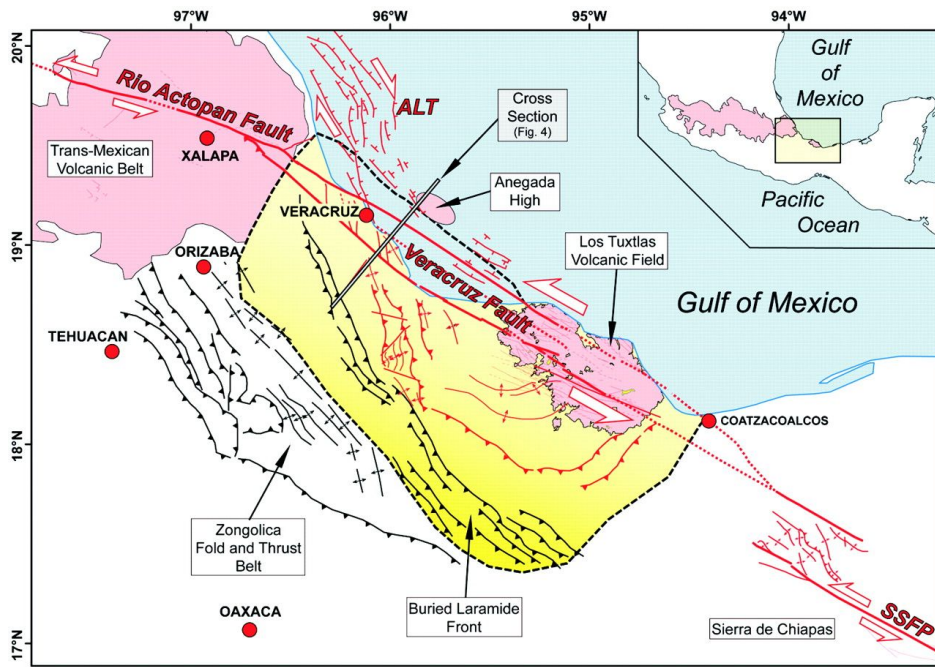


**Figure 26.** Location of the Tuxtla Volcanic Field and the Veracruz Fault (Andreani et al., 2008)



**Figure 27.** Detail of geologic structure of the Tuxtla Volcanic Field (Andreani et al., 2008)

In addition to the geologic maps that show past volcanic eruption depostion, recent hazard assessment modelling as shown in figure 28 has identified anticipated lahar mud flows from the San Martín volcano. As is apparent from all of figures 26–28, it is clear that past volcanic eruptions and

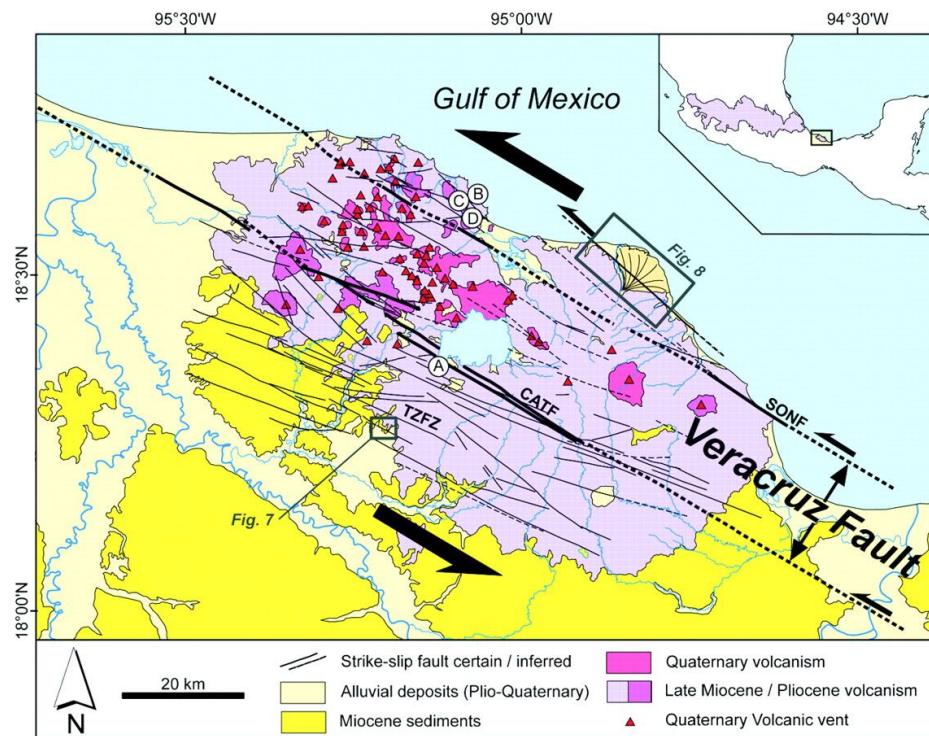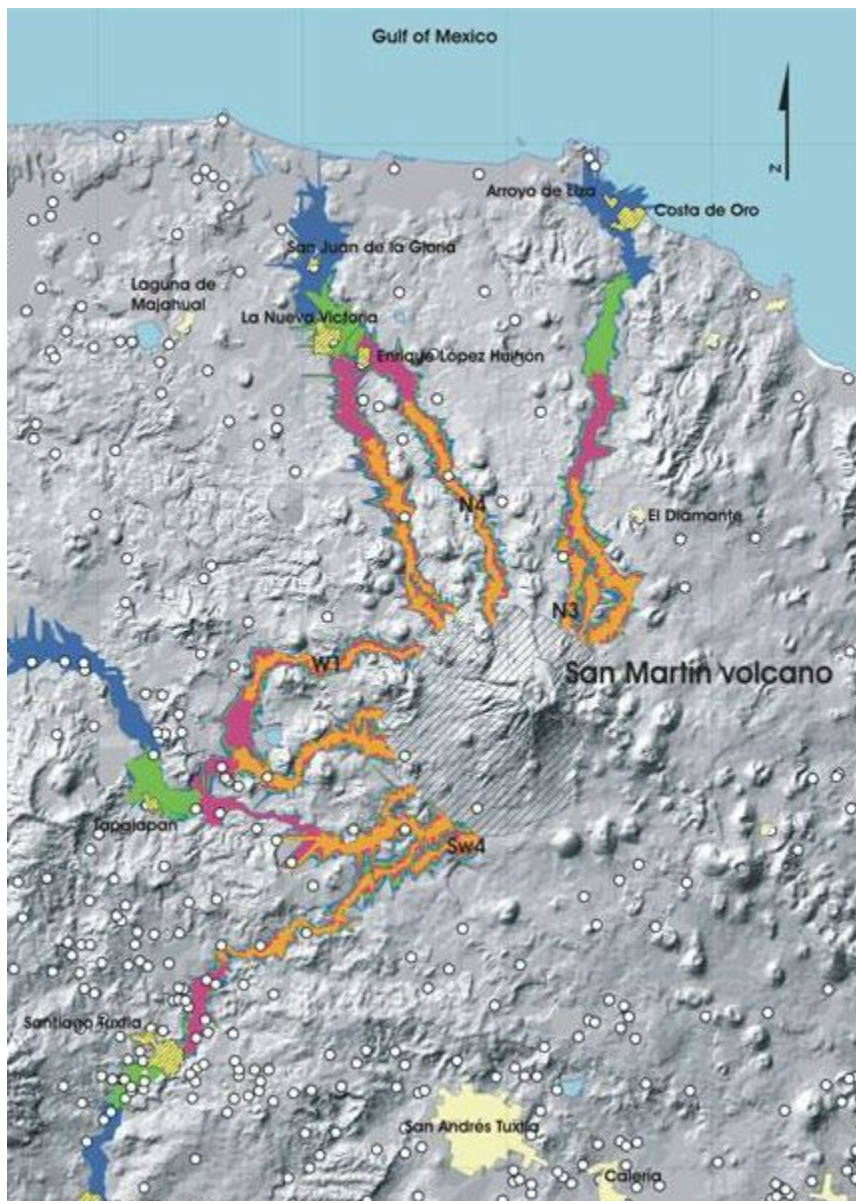lahar flows reached the Gulf of Mexico, raising the possibility of historic generation of tsunami events in the Gulf of Mexico.



**Figure 28.** Anticipated lahar flows from the San Martín volcano (Sieron et al., 2014, 290)

Eruption of San Martín in 1793

The last significant eruption of San Martín was a VEI 4 phreatomagmatic eruption in 1793. The effects and extent of the eruption were documented by Dr. Joseph Mariano Moziño. Moziño was a naturalist born and educated in New Spain. The eruption began on March 2, 1793, during the afternoon. Since heavy clouds covered the mountain and thunderstorms were frequent in its vicinity, most of the people took the explosive sounds as those of a large thunderstorm. A couple of hours later, however, the cloud cover disappeared, driven by the winds, and people were able to see:

> … a large column of fire … towards the northeast of Tuxtla and north of San Andrés; many thunderbolts stemming from its center and zigzagging in different directions,

> frightened the eyewitnesses and rushed the crowds to the temples to implore for divine mercy thinking that, if not the complete ruin of the universe, at least that of the region was inevitable. Translated from Moziño (1870, 63)

On March 3rd, explosions were heard at the villages of Perote, Teziutlan, Jalacingo, Papantla, Misantla and Andrés Chalchicomula (now Ciudad Serdán), towns located at distances as far as 300 km from the volcano, and were taken as cannonades against pirates at the port of Veracruz. More than 400 "cannon shots" were counted at Papantla and Misantla.

The second eruption, which lasted for about two days, began on May 22nd in the morning. As the wind was blowing from the north:

> The height of the fire column was much greater than the first time, with more frequent lightning, a more widespread cloud of smoke and heavier ash fallout. The sun was so much darkened that in a radius of more than 15 leagues *(83.5 kilometers)* it was necessary to use artificial lighting at noontime. Translated from Moziño (1870, 64)

By May 23<sup>rd</sup>, ashfall reached the towns of Oaxaca, Izucar, Tehuacán, Orizaba, Córdoba, and the province of Tabasco (with the principal towns then being Villahermosa and Tacotalpa). All the towns were located about 230 km and 320 km from the volcano in different directions.

A third eruption occurred on the morning of June 28th. This was the largest eruption and the southern winds carried the ash towards the sea and the hills of Tecolapan (northwest of the volcano). As a result, the roads in that area were so much disfigured that passage was impossible. Woods were set aflame during the 3 days that the eruption lasted.

In September Moziño visited the volcano and observed that the fallout was from at least 3 yards and up to 6 yards thick located in a circle around the volcano with a diameter of 2 leagues (11.1 kilometers).

In addition to the towns identified by Moziño as showing the extent of the distribution of the ash fallout, the ash from the 1793 eruption has also been identified in 2 marsh sediment cores taken about 150 km north of the El Chichón volcano (Nooren, 2009). A map showing the approximate extent of the 1793 ash distribution from volcanic eruption using this data together with the towns identified by Moziño is included as figure 29.

The description of this eruption has some interesting parallels with the account in 3<sup>rd</sup> Nephi including the onset of the eruption without warning, the initial description of the event as a storm, the zigzag-type lightening, the extremely loud continuous explosions, the ash fallout extending for hundreds of kilometers causing darkness, and the rendering of roads impassable.

**Figure 29.** The 1793 San Martín volcanic eruption estimated ash distribution

San Martín Eruptive History during Potential 3$^{rd}$ Nephi Time Frames (Smithsonian, 2014; * Nelson and Gonzalez-Caver, 1992; **Jaime-Riverón and Pool, 2009; Santley 2007; ***Santley et al., 2000)

| Start Date | Certainty | VEI | Evidence | Activity Area |
|---|---|---|---|---|
| 80 BC–320 AD | Confirmed | | Radiocarbon (uncorrected) | South flank (Cerro Puntiagudo) |
| 450 BC–150 AD | Confirmed | | Tephrochronology | South flank |
| *39 AD–410 AD | | | Radiocarbon | Carbon underneath Puntiagudo |
| **65 AD –398 AD | | | Radiocarbon | Tres Zapotes |
| **65 AD –398 AD | | | Radiocarbon | Bezuapan |
| ***50 BC–750 AD | two sigma | | Radiocarbon | Matacapan |
| ***450 BC–550 AD | two sigma | | Radiocarbon | Matacapan |
| ***850 BC–900 AD | two sigma | | Radiocarbon | Matacapan |
| ***850 BC–350 AD | two sigma | | Radiocarbon | Matacapan |
| ***850 BC–350 AD | two sigma | | Radiocarbon | Matacapan |
| ***365 BC–55 AD | uncalibrated | | Radiocarbon | Bezuapan |
| ***80 AD–680 AD | one sigma | | Radiocarbon | Bezuapan |
| ***50 AD | Confirmed | | Radiocarbon | La Joya |

Maximum recent (3000 BC to present) historical known VEI for San Martín: 4

2. Pico de Orizaba

Pico de Orizaba, also known as Citlaltépetl ("Mountain of the Star"), is Mexico's highest volcano and North America's third highest peak. Figure 30 shows it from the south. The snow-free peak at the left is Sierra Negra, a 4580-m-high Pleistocene volcano that was active simultaneously with Orizaba. Historical eruptions have consisted of moderate explosive activity and the effusion of dacitic lava flows. The latest eruption occurred during the 19th century.



**Figure 30.** Pico de Orizaba

The last major eruption of Pico de Orizaba occurred around 2150 BC, and involved the explosive disruption of a lava dome in the summit crater, forming a succession of block and ash flow and lahar deposits on the southeast and west sectors of the volcano that extend up to about 28 km from the vent. Since the last major eruption, 8 different moderate pyroclastic flow eruptions have been identified, including ash flows, scoria flows, and block and ash flows. A pyroclastic eruption relative to the 3$^{rd}$ Nephi time frame shows up in the geologic record with dated samples from 40 AD ± 40 years and 90 AD ± 40 years in the Texmalaquilla area, about 8 kilometers from the cone. A tephra fall deposit associated with an explosive eruption was reported at 140 AD ± 50 years in the San Jose area.

The extent of the volcanic deposits related to the pyroclastic eruption appears to be limited to 10 to 12 kilometers from the volcano cone. This eruption was classified as 'minor' (Höskuldsson et al., 1993) and assigned a VEI of 3.

Pico de Orizaba Eruptive History during Potential 3rd Nephi Time Frames (Smithsonian, 2014; Höskuldsson et al., 1993)

| Start Date | Certainty | VEI | Evidence | Activity Area |
|---|---|---|---|---|
| 140 ± 50 AD | Confirmed | 3 | Radiocarbon (uncorrected) | |
| 90 ± 40 AD | Confirmed | 3 | Radiocarbon (uncorrected) | |
| 40 ± 40 AD | Confirmed | 3 | Radiocarbon (uncorrected | |

Maximum recent (3000 BC to present) historical known VEI for Pico de Orizaba: 4

3. Popocatépetl

Popocatépetl, whose Aztec name means "Smoking Mountain," is a massive stratovolcano that towers more than 3200 m above the Valley of Mexico and forms North America's 2nd-highest volcano. The glacier-clad stratovolcano contains a steep-walled, 400 x 600 m wide crater. The generally symmetrical volcano is modified by the sharp-peaked Ventorrillo on the northwest, a remnant of an earlier volcano. At least three previous major cones were destroyed by gravitational failure, producing massive debris-avalanche deposits covering broad areas to the south. Three major plinian eruptions, the most recent of which took place about 800 AD, have occurred from Popocatépetl since the mid-Holocene, accompanied by pyroclastic flows and voluminous lahars that swept basins below the volcano. Frequent historical eruptions, first recorded in Aztec codices, have occurred since pre-Columbian time.

Records of the eruptions of Popocatépetl extend back to Aztec records in 1354 AD and also include Spanish Colonial records (Cruz – Reyna et al. 1995). These records do not contain a thorough accounting of any eruption to the specificity provided in the 1793 San Martín volcano eruption. An eruption in 1592 indicated that ash distribution extended 8 leagues (45 km) to Puebla, Tlaxacata, and Chalco. The distance to Tlaxacata is on the order of 50 km, but it is clear the ash extended in all directions around the volcano.

Studies of the deposits of what geologists refer to as the 200 BC eruption indicate that it included pyroclastic surges that extended up to 20 kilometers, and also included lahar flows. There are indications that stratospheric transport of the ash in this eruption occurred eastward (Macías, 2007, 202). This eruption has been characterized by archeological excavations at Tetimpa as occurring in the late part of the first century AD based on radiocarbon dating from that archeological site (Plunket et al., 1998, 292). Evidence at the site indicates that inhabitants had to flee the volcanic eruption.

**Figure 31.** Popocatépetl Volcano, December 1994

Popocatépetl Eruptive History during Potential 3$^{rd}$ Nephi Time Frames (Smithsonian, 2014; Macías, 2007; Plunket et al., 1998)

| Start Date | Certainty | VEI | Evidence | Activity Area |
|---|---|---|---|---|
| AD 240 (AD 90–395) | 2 sigma | | Radiocarbon | Tetimpa |
| 100 AD (20 BC–AD 245) | 2 sigma | | Radiocarbon | Tetimpa |
| 80 AD (91 BC–AD 315) | 2 sigma | | Radiocarbon | Tetimpa |
| 75 AD (45 BC–AD 225) | 2 sigma | | Radiocarbon | Tetimpa |
| 50 BC (357 BC–AD 116) | 2 sigma | | Radiocarbon | Tetimpa |
| 181 BC (390 BC–AD 20) | 2 sigma | | Radiocarbon | Tetimpa |
| 250 AD | Confirmed | | Radiocarbon (uncorrected) | |
| 200 BC ± 300 years | Confirmed | 4 | Radiocarbon (uncorrected) | |

Maximum recent (3000 BC to present) historical known VEI:  4

4. Other volcanoes in the land northward

The following volcanoes have been active since 3$^{rd}$ Nephi time frames, but no eruption has yet been found during the appropriate time frame. There may be some possibility that future research may identify eruptions with a suitable time frame:

- Cofre di Perote
- Chichinautzin (includes Xitle)
      Maximum recent (3000 BC to present) historical known VEI:  3

The following volcanoes have not been active since 3$^{rd}$ Nephi time frames, and for the most part have been inactive long before 3$^{rd}$ Nephi time frames. There is limited possibility that future research may identify eruptions with a suitable time frame:

- Naolinco Volcanic Field
- Los Atlixcos
- La Gloria
- Las Cumbres
- Serdan Oriental
- La Malinche
- Papayo
- Iztaccihuatl
- Nevado de Toluca
- Jocotitlán

## Volcanoes in the Land Southward

The Sorenson model does not consider geography much beyond Lake Amatitlan, as that is the southern boundary of the Land of Nephi in that model. Volcanoes in the land southward are shown in figure 32 with the exception of El Chichón, which is shown in figure 22.
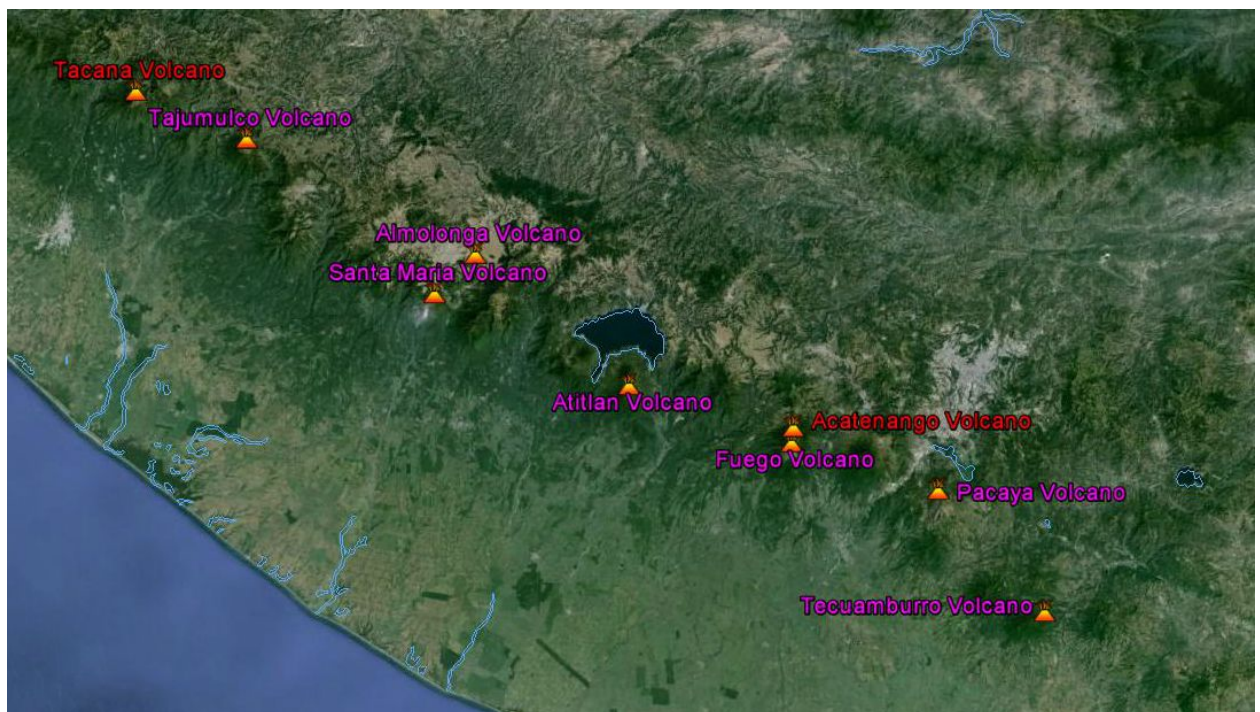


**Figure 32.** Southernmost volcanoes: red indicates active during 3$^{rd}$ Nephi time; pink indicates historically active but lacking data
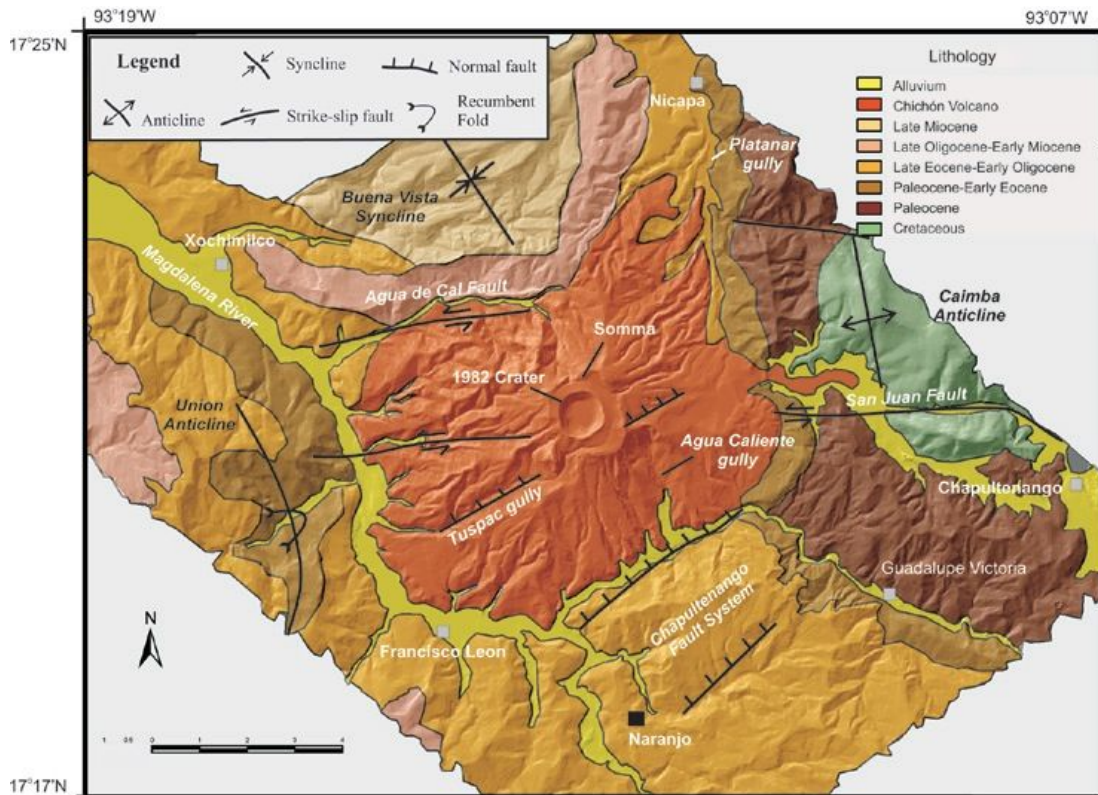
### 1. El Chichón

El Chichón is a small, but powerful tuff cone and lava dome complex that occupies an isolated part of the Chiapas region in southeast Mexico, far from other active volcanoes. Prior to 1982, this relatively unknown volcano was heavily forested and of no greater height than adjacent non-volcanic peaks. The largest dome, the former summit of the volcano, was constructed within a summit crater created

about 220,000 years ago. Two other large craters are located on the southwest and southeast flanks; a lava dome fills the southwest crater, and an older dome is located on the northwest flank. The powerful 1982 explosive eruptions of magma destroyed the summit lava dome and were accompanied by pyroclastic flows and surges that devastated an area extending about 8 km around the volcano. The eruptions created a new 1-km-wide, 300-m-deep crater that now contains an acidic crater lake (see figure 33). The El Chichón volcano, like the San Martín volcano, also occurs with a strike-slip fault cutting through it (see figure 34).



**Figure 33.** El Chichón, June 1982, two months after eruption

The volcanic deposits of El Chichón have been mapped with assignment of letters in alphabetical order going from the youngest to oldest deposits. The deposits of interest in relation to the 3$^{rd}$ Nephi time frame are the Tephra H and perhaps the Tephra G deposits. These deposits basically consist of pyroclastic flow surge deposits and ashfall. The extent of the ashfall distribution of the level VEI 5 1982 eruption is shown in figure 35 and extended over an area 425 kilometers wide.

**Figure 34.** Geologic Map of El Chichón Volcano showing strike-slip fault through the volcano (Macias, 2007)

El Chichón Eruptive History during Potential 3rd Nephi Time Frames (Smithsonian, 2014; Espíndola et al., 2000*; Nooren, 2009**)

| Start Date | Certainty | VEI | Evidence | Activity Area |
|---|---|---|---|---|
| 190 AD ± 150 years | Confirmed | | Radiocarbon (corrected) | Tephra unit G |
| 20 BC ± 50 years | Confirmed | | Radiocarbon (corrected) | Tephra unit H |
| *BC 5 (BC 114–AD 76) | 1 sigma | | Radiocarbon | Tephra unit H |
| *BC 36 (BC 191–AD 86) | 1 sigma | | Radiocarbon | Tephra unit H |
| *BC 36 (BC 191–AD 104) | 1 sigma | | Radiocarbon | Tephra unit H |
| *BC 36 (BC 191–AD 112) | 1 sigma | | Radiocarbon | Tephra unit H |
| *AD 135 (AD 75–AD 240) | 1 sigma | | Radiocarbon | Tephra unit G |
| **30 BC (120 BC–60 AD) | 1 sigma | | Radiocarbon | Tephra unit H |
| **145 BC (140 BC–150 BC) | 1 sigma | | Radiocarbon | Tephra unit H |
| **AD 95 (AD 80–AD 110) | 1 sigma | | Radiocarbon | Tephra unit G |

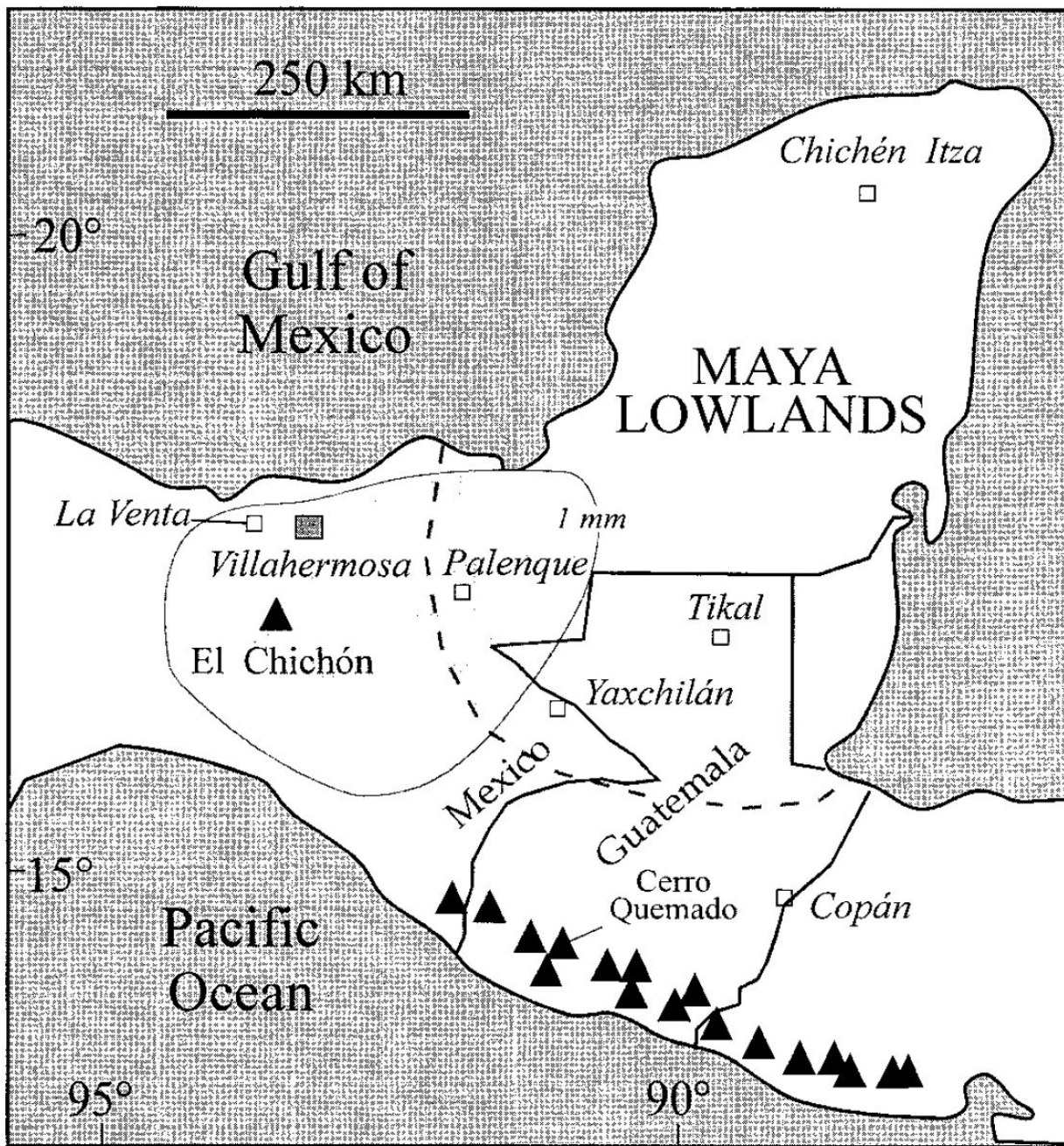Maximum recent (3000 BC to present) historical known VEI:  5

**Figure 35.** Map showing ashfall distribution from 1982 El Chichón eruption (Espíndola et al., 2000, 93)

## 2. Tacaná

Tacaná is a 4060-m-high composite stratovolcano that straddles the Mexico/Guatemala border at the Northwest end of the Central American volcanic belt (figure 36). Three large calderas breached to the south, and the elongated summit region is dominated by a series of lava domes intruded along a northeast-southwest trend. Volcanism has migrated to the southwest, and a small lava dome is located in the crater of the youngest volcano, San Antonio, on the upper southwest flank. Viscous lava flow complexes are found on the north and south flanks, and lahar deposits fill many valleys.

There is one eruption that is of interest to 3rd Nephi time frames. The eruption originated from the San Antonio volcano. This eruption produced an explosion that destroyed the summit dome, which generated pyroclastic surges and block-and-ash flow deposits that traveled 14 kilometers from the summit through ravines.



**Figure 36.** Tacaná Volcano, June 1986

Tacaná Eruptive History during Potential 3rd Nephi Time Frames (Smithsonian, 2014)

| Start Date | Certainty | VEI | Evidence | Activity Area |
|---|---|---|---|---|
| AD 70 ± 100 years | Confirmed | 4 | Radiocarbon (corrected) | San Antonio (upper SW flank) |

Maximum recent (3000 BC to present) historical known VEI:  4

3. Acatenango

Acatenango (figure 37), along with its twin volcano to the south, Volcán Fuego, overlooks the historic former capital city of Antigua, Guatemala. The first well-documented eruptions of Acatenango took place from 1924 to 1927, although earlier historical eruptions may have occurred. Francisco Vasquez, writing in 1690, noted that in 1661 a volcano that lay aside of Fuego "opened a smoking mouth and still gives off smoke from another three, but without noise."

The one eruption that occurred within the 3rd Nephi time frame principally involved ashfall tephra deposits.

**Figure 37.** Acetenango Volcano

Acetenango Eruptive History during Potential 3<sup>rd</sup> Nephi Time Frames (Smithsonian 2014; Valance 2001)

| Start Date | Certainty | VEI | Evidence | Activity Area |
|---|---|---|---|---|
| AD 90 ± 100 years | Confirmed | | Radiocarbon (uncorrected) | Pico Central |
| AD 90 ± 90 years | | | Radiocarbon | Pico Mayor |

Maximum recent (3000 BC to present) historical known VEI:  3

## 4. Other volcanoes in the land southward

The following volcanoes have been active since 3<sup>rd</sup> Nephi time frames, but no eruption has yet been found during the appropriate time frame. Care should be taken to make too many conclusions about the volcanoes listed in this section for the land southward, as very little specific research involving historical eruptions has occurred on most of these volcanoes. There may be some possibility that future research may identify eruptions with a suitable time frame for the following volcanoes:

- Tajumulco
- Santa Maria
- Almolonga
- Fuego
- Pacaya

- Tecuamburro
- Atitlán

Maximum recent (3000 BC to present) historical known VEI:  6

The following volcanoes have not been active since 3rd Nephi time frames, and for the most part have been inactive long before 3rd Nephi time frames; however, there is a lack of research on these volcanoes. There is limited possibility that future research may identify eruptions with a suitable time frame for the following volcanoes:

- Toliman
- Agua
- Cuilapa-Barbarena

## Oil and Gas Provinces

There is one potential type of earthquake byproduct, mud volcanoes, which occur exclusively in oil and gas areas, so it is important to note the extent of those areas as shown in figure 38.
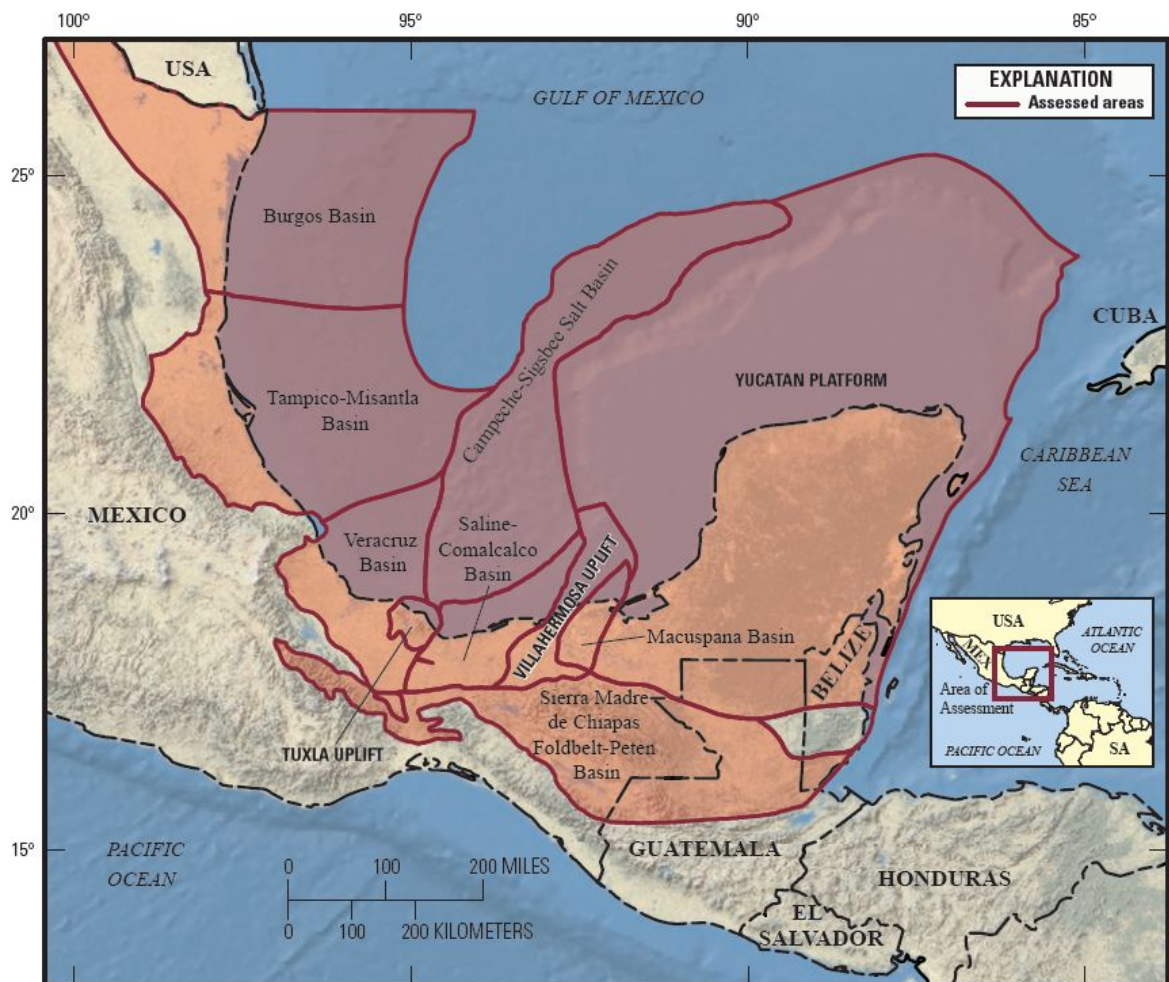


**Figure 38.** Existing and potential oil and gas provinces in the Isthmus of Tehuantepec (Schenk et al., 2012, 1)